Ferromagnetic microswimmer

M. Belovs
University of Latvia, Zellu-8, Riga LV-1002, Latvia

A. Cēbers*
Institute of Physics, University of Latvia, Salaspils-1 LV-2169, Latvia

(Received 16 February 2009; published 13 May 2009)

The self-propelling motion of the flexible ferromagnetic swimmer is described. Necessary symmetry breaking is achieved by the buckling instability at field inversion. The characteristics of self-propulsion are in good agreement with the numerical calculations of the Floquet multipliers for the ferromagnetic filament under the action of ac magnetic field. In the low frequency range the power stroke of self-propelling motion is similar to that used by the unicellular green algae chlamydomonas and in the high frequency region the self-propulsion is due to the undulation waves propagating from the free ends perpendicularly to ac magnetic field.

DOI: 10.1103/PhysRevE.79.051503 PACS number(s): 83.80.Gv, 47.63.Gd, 46.25.Hf

I. INTRODUCTION

The current trend of miniaturization has caused interest in the creation of microdevices which can perform mechanical work [1]. Rather promising is creation of artificial microswimmers which may be manipulated by the external electromagnetic field [2]. The symmetry breaking necessary for the creation of the thrust is achieved by attaching the cargo to the one of the ends of the filament [2] or by using buckling instability of the superparamagnetic filaments in the magnetic field [3,4]. The locomotion of these filaments is produced by the propagating undulation waves, which propel the filament in the direction of free ends [5,6]. Different numerical models are developed recently for the study of the locomotion of flexible superparamagnetic filaments [7,8].

A new type of the magnetic flexible filaments is created recently by linking the core-shell ferromagnetic particles [9] by 1000 bp long DNA fragments [10]. Although the length of the ferromagnetic filaments synthesized so far is not very large (about 10–15 linked ferromagnetic particles with a diameter 4 μm) nevertheless these filaments exhibit the behavior predicted for the semiflexible ferromagnetic filaments—development in dependence on initial conditions of *S*- or *U*-like deformation modes at the magnetic-field inversion and orientation perpendicularly to the high frequency ac magnetic field [11].

The value of the magnetoelastic number Cm of the ferromagnetic filaments for magnetic-field strength applied in [10] is about 10. This allows us to expect that the ferromagnetic filaments should be interesting for the creation of microswimmers. Buckling modulus of ferromagnetic filaments C was estimated from these experiments as 10^{-12} erg cm. Since the persistence length $l_p = C/k_BT$ is large then thermal fluctuations of these filaments are not important. Here we are giving the theoretical results on the characteristics of microswimmers built by using these ferromagnetic filaments. It may be interesting to remark that thermal fluctuation effects are important for the chains of the ferromagnetic nanoparticles which persistence length may be estimated by $l_p = \lambda d/2$ [12] ($\lambda = m^2/d^3k_BT$ is magnetodipolar interaction parameter of these particles with magnetic moment m and diameter d). Investigation of working of nanomachines formed by ferromagnetic nanoparticles is pending for future publications.

II. MODEL

Equations for the superparamagnetic and ferromagnetic filaments are derived in [4,11]. Here we are considering two-dimensional case. The tangent and normal vectors are $\vec{\tau} = (\cos\vartheta, \sin\vartheta)$; $\vec{n} = (-\sin\vartheta, \cos\vartheta)$, where ϑ is the angle between the tangent and the external field $\vec{H} = (-\cos\omega t, 0)$ (Fig. 1). The curvature of the filament $1/R$ reads $1/R = -d\vartheta/dl$ (l is the arclength of center line). The normal and tangential components of the stress are (here and further subscript,… denotes the derivative)

$$F_n = C\left(\frac{1}{R}\right)_{,l} - M\vec{H}\cdot\vec{n} \tag{1}$$

and

$$F_\tau = -C\frac{1}{2R^2} - \Lambda. \tag{2}$$

Here C is bending modulus, M is the magnetization of filament per unit length that is parallel to the tangent vector, $\vec{H}$ is the strength of applied magnetic field, and Λ is the Lagrange multiplier enforcing inextensibility of the filament.

To have self-propulsion it is necessary to take into account in the theoretical model the anisotropy of the hydrodynamic drag. In this case the velocity components in the direction of the normal and tangent of the filament are

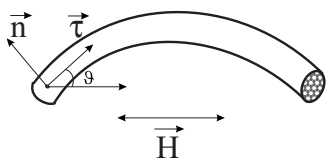

FIG. 1. Picture of a ferromagnetic filament.

*aceb@tesla.sal.lv

$$v_n = \frac{1}{\zeta_\perp}\left(F_{n,l} - \frac{1}{R}F_\tau\right), \tag{3}$$

$$v_\tau = \frac{1}{\zeta_\parallel}\left(F_{\tau,l} + \frac{1}{R}F_n\right). \tag{4}$$

Here $\zeta_\perp$ and $\zeta_\parallel$ are the drag coefficients in the case of motion perpendicular and parallel to the local element of the filament, respectively. In the case of slender prolate spheroid of major axis a and minor axis b these coefficients may be estimated by $\zeta_\perp = 4\pi\eta/[\log(2a/b)+1/2]$ and $\zeta_\parallel = 2\pi\eta/[\log(2a/b)-1/2]$ [13].

Using the relation

$$\frac{d\vartheta}{dt} = v_{n,l} - \frac{1}{R}v_\tau,$$

scaling the arclength by L ($2L$ is the length of the filament), time by the characteristic elastic relaxation time $\tau_e = \zeta_\perp L^4/C$, stress by C/L^2 and introducing the magnetoelastic number $\mathrm{Cm} = MHL^2/C$ the equation for the tangent angle in the ac magnetic field ($\tilde{\omega} = L^4/L_e^4$ is dimensionless frequency of applied field, $L_e = (C/\omega\zeta_\perp)^{1/4}$ is elastic penetration length [14], tildes are further omitted) reads

$$\vartheta_{,t} = -\vartheta_{,llll} - \frac{1}{2}(\vartheta_{,l})^3_{,l} - \mathrm{Cm}\cos\omega t(\sin\vartheta)_{,ll} - (\vartheta_{,l}\Lambda)_{,l}$$

$$-\frac{\zeta_\perp}{\zeta_\parallel}\vartheta_{,l}(\Lambda_{,l} - \vartheta_{,l}\mathrm{Cm}\cos\omega t\sin\vartheta). \tag{5}$$

Equation for the Lagrange multiplier Λ enforcing inextensibility $\vec{t}\cdot\vec{v}_{,l} = 0$ reads

$$(\vartheta_{,l})^2\Lambda - \frac{\zeta_\perp}{\zeta_\parallel}\Lambda_{,ll} + \frac{1}{2}(\vartheta_{,l})^4 + \vartheta_{,l}\vartheta_{,lll}$$

$$+\frac{\zeta_\perp}{\zeta_\parallel}\mathrm{Cm}\cos\omega t(\vartheta_{,l}\sin\vartheta)_{,l} + \vartheta_{,l}\mathrm{Cm}\cos\omega t(\sin\vartheta)_{,l} = 0. \tag{6}$$

Since the torque acting in the cross section of the filament is $-C/R$ [4] then at the unclamped ends of the filament its curvature is equal to zero. Then Eqs. (1) and (2) in the case of free ends of filament ($F_n = F_\tau = 0$) give the set of boundary conditions:

$$\vartheta_{,l}|_{l=\pm1} = 0,$$

$$\Lambda|_{l=\pm1} = 0,$$

$$(\vartheta_{,ll} + \mathrm{Cm}\cos\omega t\sin\vartheta)|_{l=\pm1} = 0. \tag{7}$$

The linear stability analysis of this model in the case of static field is carried out in [11]. Essential for the creation of the microswimmer is the fact that at $\mathrm{Cm} > \pi^2/4$ (magnetization of straight filament is opposite to the field) besides the unstable S-like deformation mode, which exists for all Cm values and which corresponds to the overturning of the filament at the magnetic-field inversion, there is growing U-like deformation mode. The increment of U-like mode becomes equal to the increment of S-like mode at $\mathrm{Cm} = (n\pi)^2/3$, $n = 1,2,\ldots$ [11]. Thus we expect that the ferromagnetic swimmer is possible at $\mathrm{Cm} > \pi^2/3$. Development of this mode for large Cm values leads to the formation of the loop which breaks the symmetry with a respect to the reflection in the plane of motion [15]. It should be mentioned that this shape similarly to the hairpin formed by the superparamagnetic filaments in the perpendicular field [3,4] is metastable. However the characteristic time of the development of the instability of the loop which consists in its translation to the one of the ends of the filament is exponentially small for the large magnetoelastic numbers.

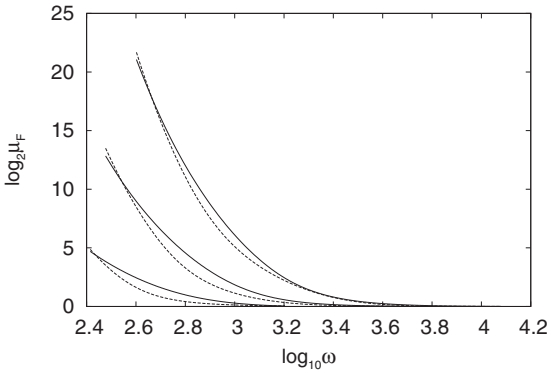

FIG. 2. Floquet multipliers of ferromagnetic filament as function of frequency. Solid lines—U-like mode, dashed lines—S-like mode. Cm is decreasing in direction from upper curves to lower curves: Cm=72;52;35.

III. SELF-PROPULSION

The symmetry breaking at the loop formation is used further for the construction of the ferromagnetic microswimmer. For this it is necessary that the shape with the broken reflectional symmetry exists in ac magnetic field. As a criterion for the choice of the values of the physical parameters where this takes place the Floquet multipliers μ_F for the linearized equations and boundary conditions [Eqs. (5)–(7)] are calculated numerically by finding the eigenvalues of the linear operator A giving the solution after the period: $\vartheta|_{t=T} = A\vartheta|_{t=0}$; $T = 2\pi/\omega$. Only the modes corresponding to the eigenvalues of A (Floquet multipliers) greater than 1 are important in the long time limit. Numerical calculations show that only two modes have the Floquet multipliers greater than 1. These modes correspond to U- and S-like deformation modes of the filament. Values of their Floquet multipliers for several values of the magnetoelastic number are shown in Fig. 2.

Since the algorithm used for the calculation of the shape of the filament gives the tangent angle and thus the shape of the filament up to arbitrary displacement in space an additional equation for the calculation of the position of the mass center is necessary. Equations (3) and (4) for the velocity of the local element of the filament give

$$\vec{v} = \frac{1}{\zeta_\perp}\vec{F}_{,l} + \left(\frac{1}{\zeta_\parallel} - \frac{1}{\zeta_\perp}\right)\left(F_{\tau,l} + \frac{1}{R}F_n\right)\vec{\tau}. \tag{8}$$

Since the force applied to the ends of the filament is zero relation (8) gives

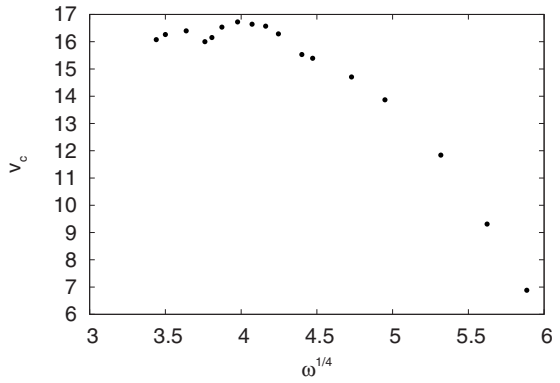

FIG. 3. Velocity of ferroswimmer in dependence on ratio of the length of filament to the elastic penetration length. Cm=35.

$$\zeta_\perp 2L\vec{v}_c = \left(\frac{\zeta_\perp}{\zeta_\parallel} - 1\right)\int_{-L}^{L}\left(F_{\tau,l} + \frac{1}{R}F_n\right)\vec{\tau}dl. \tag{9}$$

In dimensionless variables after integration by parts we have

$$\frac{dx_c}{dt} = \frac{1}{2}\left(\frac{\zeta_\perp}{\zeta_\parallel} - 1\right)\left\{-\mathrm{Cm}\cos(\omega t)\cos^2\vartheta\Big|_{-1}^{+1} - \int_{-1}^{+1}[\Lambda + \mathrm{Cm}\cos(\omega t)\cos\vartheta]\sin\vartheta\cdot\vartheta_{,l}dl\right\}, \tag{10}$$

$$\frac{dy_c}{dt} = \frac{1}{2}\left(\frac{\zeta_\perp}{\zeta_\parallel} - 1\right)\left\{-\mathrm{Cm}\cos(\omega t)\cos\vartheta\sin\vartheta\Big|_{-1}^{+1} + \int_{-1}^{+1}[\Lambda + \mathrm{Cm}\cos(\omega t)\cos\vartheta]\cos\vartheta\cdot\vartheta_{,l}dl\right\}. \tag{11}$$

As we see from Fig. 2 there is limited range of the frequency where the Floquet multiplier of the *U*-like mode is greater than for the *S*-like mode. In this range of the frequency we should expect the existence of the steady oscillation regime of the filament and due to the symmetry breaking its propulsion. The *S*-like mode is symmetric and does not imply self-propulsion.

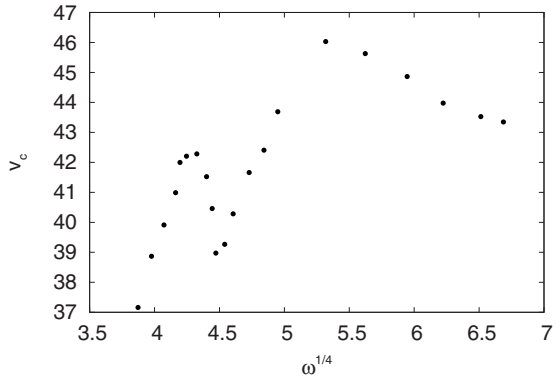

FIG. 4. Velocity of ferroswimmer in dependence on ratio of the length of filament to the elastic penetration length. Cm=72.

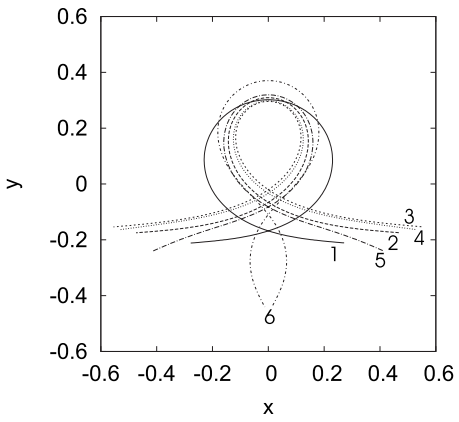

FIG. 5. Power stroke of ferroswimmer. Dimensionless time: 0.3153(1); 0.3167(2); 0.3181(3); 0.3194(4); 0.3208(5); 0.3222(6). ω=300; Cm=72. Positions of center of mass for configurations 1–6 are shown by black dots in Fig. 7.

Numerical calculations carried out agree with these expectations as it is illustrated by Figs. 3 and 4, where the velocity of microswimmer is shown in dependence on the frequency. As an initial configuration for the dynamics of swimmer at given value of Cm the loop formed at field inversion from the slightly perturbed straight configuration with a tangent angle $\vartheta = -0.01\sin(\pi l/2)$ is taken. We can remark that the same values of the velocity of self-propulsion are obtained starting directly from the slightly perturbed straight configuration with a tangent angle $\vartheta = -0.01\sin(\pi l/2)$. For frequencies lower than shown in Figs. 3 and 4 after some transition period *S*-like deformation mode of the filament develops and its self-propelling motion stops.

Rather interesting is the mechanism of generation of the self-propelling force by the ferromagnetic filament. The dynamics of shapes of the filament in the set of coordinates connected with its center of mass is shown in Figs. 5 and 6. In the initial stage of power stroke (Fig. 5) the tip of the loop

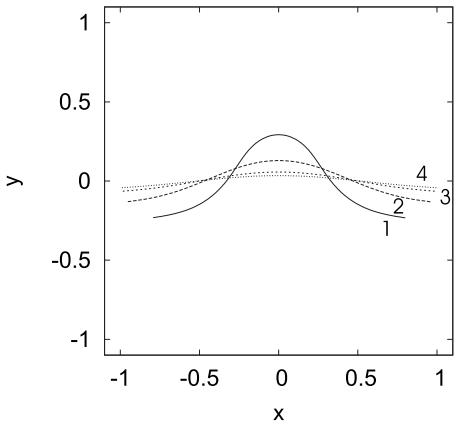

FIG. 6. Return stroke of ferroswimmer. Dimensionless time: 0.3250(1); 0.3264(2); 0.3278(3); 0.3292(4). ω=300; Cm=72. Positions of center of mass for configurations 1–4 are shown by white dots in Fig. 7.

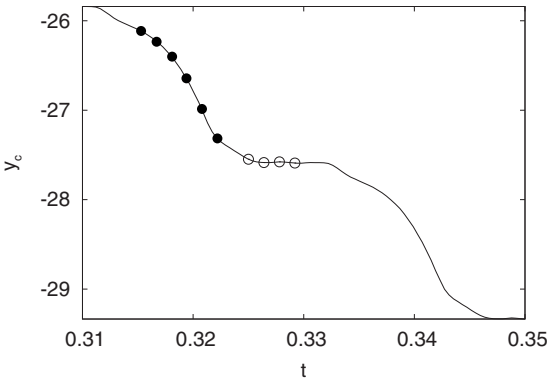

FIG. 7. Coordinate of mass center as function of time for time interval corresponding to dynamics shown in Figs. 5 and 6. Black circles—power stroke, white circles—return stroke. ω=300; Cm=72.

remains practically motionless but its legs move upward and create the force on the filament downward. The force generation in this stage is rather similar to the mechanism of self-propulsion by the unicellular green algae chlamydomonas [16,17]. In the return stroke phase (Fig. 6) tip and the legs of loop move in the opposite directions preparing the breaststroke and the filament remains practically motionless. The displacements of the center of mass of the filament during the power and return strokes for two periods can be seen in Fig. 7. Similar sequence of events for other value of magnetoelastic number is shown in Figs. 8 and 9. The displacements of the center of mass during the power and return strokes for two periods are shown in Fig. 10.

Several maxima for the frequency dependence of the velocity of swimmer (Figs. 3 and 4) allow us to presume several mechanisms of the generation of the self-propelling force by the ferromagnetic filament. In low frequency regime we see the power stroke, where the force is generated by rather long extremities of the swimmer (configurations 1–3 in Fig. 5). For high frequency region as illustrated by Fig. 11 an important role in the force generation is played by the wave propagating from the free end of the filament to its tip.

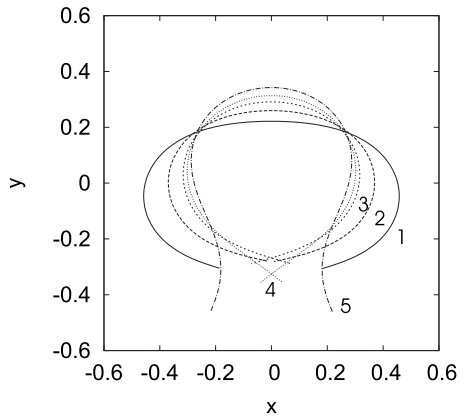

FIG. 8. Power stroke of ferroswimmer. Dimensionless time: 0.3222(1); 0.3229(2); 0.3236(3); 0.3243(4); 0.3250(5), ω=800; Cm=72. Positions of center of mass for configurations 1–5 are shown by black dots in Fig. 10.

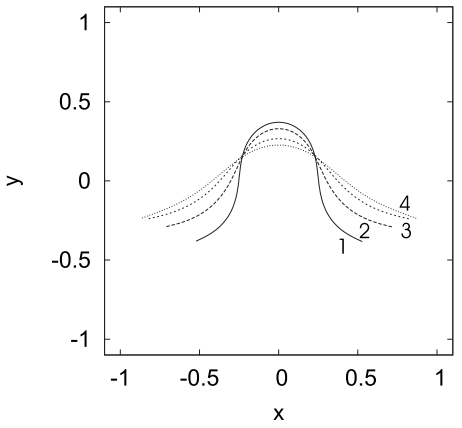

FIG. 9. Return stroke of ferroswimmer. Dimensionless time: 0.3257(1); 0.3264(2); 0.3271(3); 0.3278(4), ω=800; Cm=72. Positions of center of mass for configurations 1–4 are shown by white dots in Fig. 10.

This can be illustrated by the solution of the following problem.

Let us consider the semi-infinite ferromagnetic filament at $x \in [-\infty;0]$ under the action of perpendicular ac magnetic field. Since according to Eq. (1) the magnetic term in the stress is constant then partial differential equation for the displacement of the filament $y(x,t)$ in the direction of the magnetic field is

$$\zeta_\perp y_{,t} = -Cy_{,xxxx}. \tag{12}$$

It should be solved at boundary conditions corresponding to the free and unclamped end

$$y_{,xx}(0,t) = 0,$$

$$Cy_{,xxx}(0,t) = -MH\cos(\omega t), \tag{13}$$

and condition at far end of the filament: $y \to 0$ at $x \to -\infty$. Solution of the problem reads

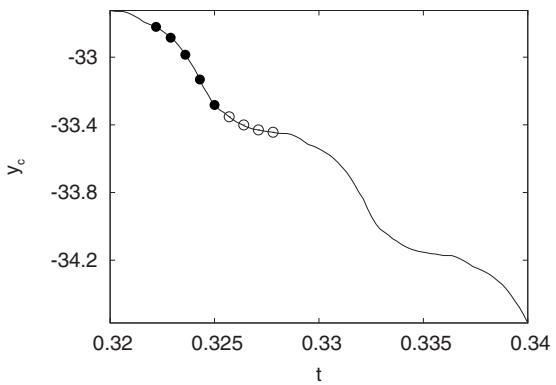

FIG. 10. Coordinate of mass center as function of time for time interval corresponding to dynamics shown in Figs. 8 and 9. Black circles—power stroke, white circles—return stroke. ω=800; Cm=72.

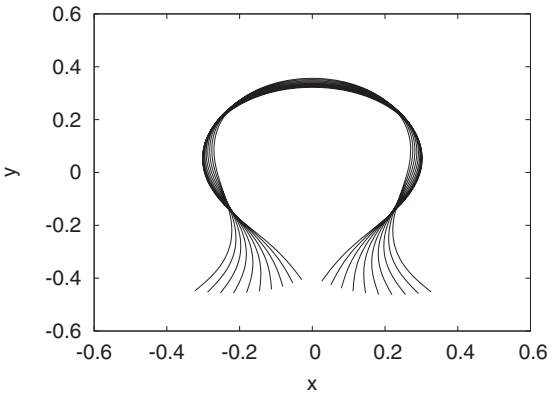

FIG. 11. Configurations of swimmer in last stage of power stroke for time interval [0.3246; 0.3252]. In this time interval ends of filament move outward. $\omega=800$; Cm=72.

$$y = y_0\{\exp[\cos(3\pi/8)x/L_e]\cos[\omega t + \sin(3\pi/8)x/L_e - 3\pi/8] + \exp[\cos(\pi/8)x/L_e]\cos[\omega t - \sin(\pi/8)x/L_e - 3\pi/8]\}. \quad (14)$$

Here

$$y_0 = \frac{MHL_e^3}{\sqrt{2}C}.$$

Solution given by relation (14) describes two counterpropagating waves with different rates of decay at $x \to -\infty$. Since wave propagating to free end decays faster the propagating in the negative x axis direction wave arises.

According to the relation for the self-propulsion force ($\langle\ \rangle$ denotes time average with respect to the period of the field) [18]

$$F = (\zeta_\perp - \zeta_\parallel)\left\langle \int_{-\infty}^{0} y_{,t} y_{,x} dx \right\rangle \quad (15)$$

we conclude that the self-propelling force acts in the direction opposite to the direction of wave propagation, that is in the direction of the free end of the filament. It is situation that is observed in numerical experiments—the filament moves perpendicularly to the magnetic field in the direction of its free ends.

Let us give some estimates for the parameters of microswimmers that can be expected for real ferromagnetic filaments. Ferromagnetic filaments are studied in [10] and for 31 μm long filament the value of magnetoelastic number Cm approximately equal to 11 at field strength 28 Oe is obtained. Using the magnetic properties of the core shell ferromagnetic particles determined in [9] the bending modulus of the ferromagnetic filaments C is estimated as 10^{-12} erg cm. Using the relation for the drag coefficient $\zeta_\perp = 4\pi\eta/[\ln(2L/r)+1/2]$ (r is radius of particles, η is viscosity, which should be taken equal to the viscosity of water since the synthesis of the ferromagnetic filaments occurs in water solutions of DNA) the expected optimal frequency of ac field $\omega_o/2/\pi[(\omega_o\tau_e)^{1/4} \simeq 4]$ is approximately 200 Hz. The velocity of swimmer depends on Cm. For the particular case shown in Fig. 3 the estimated velocity of the swimmer is approximately 1.2 mm/s. The corresponding hydrodynamic drag is about 150 pN. These estimates show that creation of the microswimmer on the basis of ferromagnetic filaments is quite realistic.

IV. CONCLUSIONS

We have attempted to show that ferromagnetic filaments can be used for the construction of microswimmers. Necessary symmetry breaking for the self-propulsion of the filament is created by the buckling instability. Frequency range where self-propulsion is operative correlates with the frequency range where the Floquet multiplier of U-like deformation mode is the largest. Frequency dependence of the velocity of self-propulsion indicates on several mechanisms of self-propulsion—in the low frequency regime the power stroke resembles the power stroke of the unicellular green algae chlamydomonas and in the high frequency regime the power stroke is created by the undulation waves propagating from the free ends of the filament perpendicularly to ac magnetic field.

[1] E. R. Kay, D. A. Leigh, and F. Zerbetto, Angew. Chem. Int. Ed. **46**, 72 (2007).
[2] R. Dreyfus *et al.*, Nature (London) **437**, 862 (2005).
[3] C. Goubault, P. Jop, M. Fermigier, J. Baudry, E. Bertrand, and J. Bibette, Phys. Rev. Lett. **91**, 260802 (2003).
[4] A. Cēbers, J. Phys.: Condens. Matter **15**, S1335 (2003).
[5] A. Cēbers, Magnetohydrodynamics **41**, 63 (2005).
[6] M. Roper, R. Dreyfus, J. Baudry, M. Fermigier, J. Bibette, and H. A. Stone, J. Fluid Mech. **554**, 167 (2006).
[7] E. Gauger and H. Stark, Phys. Rev. E **74**, 021907 (2006).
[8] E. E. Keaveny and M. R. Maxey, J. Fluid Mech. **598**, 293 (2008).
[9] J. Connoly, T. G. St. Pierre, and J. Dobson, Bio-Medical Mater. Des. **15**, 421 (2005).
[10] K. Ērglis, M. Belovs, and A. Cēbers, JMMM **321**, 650 (2009).
[11] M. Belovs and A. Cēbers, Phys. Rev. E **73**, 051503 (2006).
[12] A. Cēbers, Curr. Opin. Colloid Interface Sci. **10**, 167 (2005).
[13] J. Happel and H. Brenner, *Low Reynolds Number Hydrodynamics* (Prentice-Hall, Englewood Cliffs, NJ, 1965).
[14] C. H. Wiggins and R. E. Goldstein, Phys. Rev. Lett. **80**, 3879 (1998).
[15] A. Cēbers and T. Cīrulis, Phys. Rev. E **76**, 031504 (2007).
[16] D. L. Ringo, J. Cell Biol. **33**, 543 (1967).
[17] D. Bray, *Cell Movements* (Garland, 2001).
[18] E. Lauga and Th. R. Powers, e-print arXiv:0812.2887.